2014 IEEE 34th International Scientific Conference on ELECTRONICS AND NANOTECHNOLOGY (ELNANO)

National Technical University of Ukraine
"Kyiv Polytechnic Institute"

CONFERENCE PROCEEDINGS

April 15-18, 2014
Kyiv, Ukraine

2014 IEEE XXXIV International Scientific Conference Electronics and Nanotechnology (ELNANO)

$(1\text{-}x)BaTiO_3$–$x(Li_{0.5}Bi_{0.5})TiO_3$ PTCR Solid Solution

T.A.Plutenko, O.I.V'yunov, A.G.Belous
Department of Solid State Chemistry
Vernadskii Institute of General and Inorganic Chemistry NASU
Kyiv, Ukraine
vyunov@ionc.kiev.ua

Darko Makovec
Department for Materials Synthesis,
Jozef Stefan Institute,
Ljubljana, Slovenia
darko.makovec@ijs.si

***Abstract* — $(1\text{-}x)BaTiO_3$–$xLi_{0.5}Bi_{0.5}TiO_3$ ($0 \leq x \leq 0.6$) based solid solutions were synthesized by solid state reaction technique. Materials were sintered in reducing atmosphere in the temperature range 1200-1400°C with subsequent oxidation in air at 700°C. Intermediate phases formed during synthesis of solid solutions were defined. It was shown that the change in the unit cell parameters of $(1\text{-}x)BaTiO_3$–$xLi_{0.5}Bi_{0.5}TiO_3$ solid solutions obeys Vegard's law. It was determined that at room temperature lithium-bismuth titanate is unstable and has cubic symmetry. It was found that lithium-bismuth titanate and barium titanate based solid solutions exhibit a positive temperature coefficient of resistance (PTCR). With increasing of lithium-bismuth titanate content in $(1\text{-}x)BaTiO_3$–$xLi_{0.5}Bi_{0.5}TiO_3$, the minimum resistance value in the PTCR region increases, Curie temperature of solid solutions does not change, while the maximum of dielectric permittivity becomes diffused.**

Keywords — Lead-free; PTCR; EDX; impedance spectroscopy.

I. INTRODUCTION

Barium titanate is ferroelectric material with high dielectric constant and is used in the manufacture of multilayer capacitors, thermistors and piezoelectric transducers [1]. It is known that the donor doped barium titanate $(Ba,Y)TiO_3$ is used in self-regulating heaters, current limiters due to the appearance above the Curie temperature T_C (120ºC for $BaTiO_3$) effect of the positive temperature coefficient of resistance (PTCR) [2,3]. This effect is originated from the presence of semiconducting properties in core and dielectric properties at boundaries of ferroelectric ceramic grain. It is known that the addition of potassium-bismuth titanate $K_{0.5}Bi_{0.5}TiO_3$ [4] and sodium-bismuth titanate $Na_{0.5}Bi_{0.5}TiO_3$ [5] to barium titanate shifts the Curie temperature toward the higher values and reduces the formation and sintering temperatures of solid solutions, but there is no information in the literature about effect of lithium-bismuth titanate $Li_{0.5}Bi_{0.5}TiO_3$ on barium titanate properties. Despite the fact that $Li_{0.5}Bi_{0.5}TiO_3$ wasn't synthesized it has been used as a component of solid solution $[Bi_{0.5}(Na_{1-x-y}K_xLi_y)_{0.5}]\{Ti,Nb\}O_3$ in order to reduce sintering temperature, porosity and improve piezoelectric properties [6,7]. Information about the influence of $Li_{0.5}Bi_{0.5}TiO_3$ in these systems is contradictory: with increase in lithium-bismuth titanate, Curie temperature is increased according [8,9], and decreased according [3].

It is known that synthesis of barium titanate based solid solutions is a multistep process. Knowledge of the phase transformations sequence during synthesis is necessary in order to optimize the production process of materials. Intermediate phases $BaTi_3O_7$, β-$BaCO_3$, Ba_2TiO_4, $BaTi_4O_9$ are formed during synthesis of barium titanate $BaTiO_3$ from barium carbonate and titanium oxide [10]. It is also known that phases Li_4TiO_4, Li_2TiO_3, $Li_4Ti_5O_{12}$, Li_2TiO_3 and $Li_2Ti_3O_7$ are formed by heating a mixture of powders Li_2CO_3 and TiO_2 in the temperature range 800-1150°C [11]. But there are no published data about single phase $Li_{0.5}Bi_{0.5}TiO_3$ and about the sequence of the chemical reactions during the synthesis of $(1\text{-}x)BaTiO_3$–$xLi_{0.5}Bi_{0.5}TiO_3$ solid solutions.

The aim of this work is the synthesis, study of the structure, electrical properties and the sequence of phase transformations during the synthesis of solid solutions $(1\text{-}x)BaTiO_3$–$xLi_{0.5}Bi_{0.5}TiO_3$.

II. EXPERIMENTAL DETAILS

Solid solutions $(1\text{-}x)BaTiO_3$-$xLi_{0.5}Bi_{0.5}TiO_3$ ($0 \leq x < 0.6$) were prepared by solid state reaction technique. Li_2CO_3, $BaCO_3$, Bi_2O_3 and TiO_2 were used as the starting reagents. The powders were mixed for 4 hours in the presence of ethanol in a ball mill. Dried at 100-120ºC powders were sieved through a nylon sieve. Samples were synthesized in the temperature range 970-1000°C for 4 hours. The powders of solid solutions were pressed using a 5% polyvinyl alcohol into tablets (10 mm in diameter and 2 mm thickness) at a pressure of 150 MPa. Tablets were sintered in the gas mixture N_2/H_2 (99.5:0.5) at 1200-1400ºC with subsequent oxidation in air at 700°C. The phases were characterized by X-ray powder diffractometry (XRPD) using DRON-4-07 diffractometer (Cu Kα radiation; 40 kV, 20 mA). The lattice parameters were refined by the Rietveld fullprofile analysis. XRPD patterns were collected in the range 2θ = 10-150° in step-scan mode with a step size of $\Delta 2\theta$ = 0.02° and a counting time of 6 s per data point.

As external standards, we used SiO_2 (for 2θ) and Al_2O_3 NIST SRM1976 (for the intensity). The temperature dependence of the electrical resistance of the samples was measured in the temperature range 20°C to 400°C. Impedance data were obtained using a 1260 Impedance / Gain-phase Analyzer (Solartron Analytical) in the range 100 Hz to 1 MHz. Microstructure of ceramic samples was analyzed with a transmission electron microscope (JEOL in 2100), equipped with an energy dispersive X-ray spectrometer operated at 200 kV and scanning electron microscopy Jeol JSM 6510.

III. RESULTS AND DISCUSSION

Calculations of unit cell parameters using the Rietveld full-profile analysis (Fig. 1) showed that in the $(1\text{-}x)BaTiO_3$–$xLi_{0.5}Bi_{0.5}TiO_3$ system solid solutions are formed in the range

978-1-4799-4580-1/14/$31.00 ©2014 IEEE

$0 \le x \le 0.6$ (Fig. 2). In this range, double peak corresponding to 002 and 200 planes is gradually transformed into a singlet corresponding to the 200 plane (inset in Fig. 2). This dependence is caused by the fact that the structure of the solid solution (1-x)$BaTiO_3$-$xLi_{0.5}Bi_{0.5}TiO_3$ in the concentration range of $0 \le x < 0.5$ is tetragonal, while at higher concentrations the lithium-bismuth titanate $0.5 \le x \le 0.6$ structure becomes cubic (Fig. 3). Change in the unit cell parameters (Fig. 3) obeys the Vegard's law, the unit cell volume with increasing x decreases due to the lower values of the average ionic radius in barium site. With increasing of lithium-bismuth titanate content $x > 0.6$ peaks of additive phases ($Bi_4Ti_3O_{12}$, $Bi_2Ti_2O_7$, $Li_4Ti_5O_{12}$) appears (Fig. 3).

To characterize the stability of the ABO_3 perovskite structure, some steric parameters are used, in particular, Goldschmidt tolerance factor t:

$$t1 < t = \frac{\overline{R}_A + R_O}{\sqrt{2}(\overline{R}_B + R_O)} < t2 \qquad (1)$$

where $\overline{R}_A$ is the average value of the radius in the A site; t, t_1 and t_2 are tolerance factors. Experimental data show that a stable perovskite structure is formed at $0.84 < t < 1.07$ [12].

Using the formula (1), steric parameters were calculated in order to determine the stability of the perovskite structure in the system (1-x)$BaTiO_3$–$xLi_{0.5}Bi_{0.5}TiO_3$. Shannon ionic radii were used for calculation.

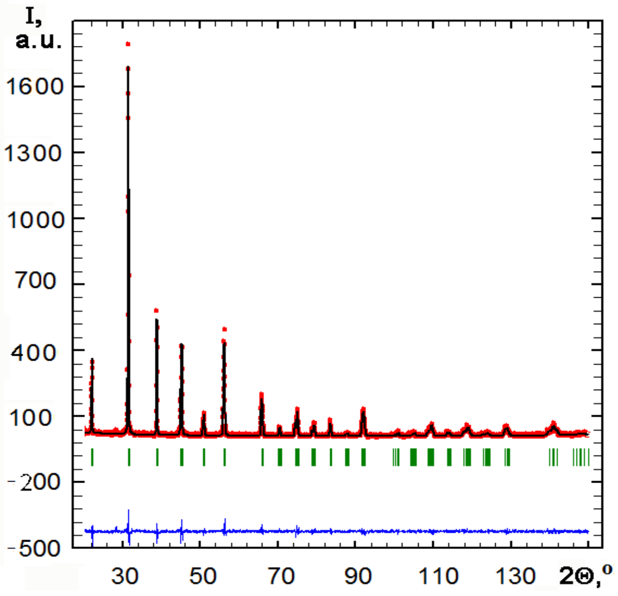

Fig. 1. Experimental (points) and calculated (line) diffraction patterns at room temperature the solid solution (1-x)$BaTiO_3$-$xLi_{0.5}Bi_{0.5}TiO_3$, where x=0.1.

According to the calculations, the solid solutions of (1-x)$BaTiO_3$–$xLi_{0.5}Bi_{0.5}TiO_3$ with perovskite structure can be formed in limited range $0 \le x \le 0.8$. Thus, the individual compound $Li_{0.5}Bi_{0.5}TiO_3$ is unstable at room temperature due to steric limitations. Despite the fact that an individual compound $Li_{0.5}Bi_{0.5}TiO_3$ cannot be obtained, the structure of lithium-bismuth titanate can be stabilized by formation of (1-x)$BaTiO_3$–$xLi_{0.5}Bi_{0.5}TiO_3$ solid solution. By extrapolation of the dependences of unit cell parameters in the system (1-x)$BaTiO_3$–$xLi_{0.5}Bi_{0.5}TiO_3$ to x=1, the value for the cubic unit cell of $Li_{0.5}Bi_{0.5}TiO_3$ was obtained (a = 4.00126 Å).

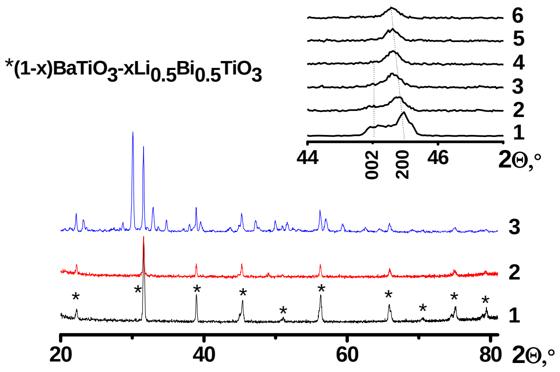

Fig. 2. Diffraction patterns of (1-x)$BaTiO_3$–$xLi_{0.5}Bi_{0.5}TiO_3$ solid solutions, x=0.1 (1) 0.6 (2) 0.7 (3). Inset: Change in peaks planes 002 and 200 of (1-x)$BaTiO_3$–$xLi_{0.5}Bi_{0.5}TiO_3$ solid solutions, x = 0 (1) 0.1 (2) 0.2 (3) 0.3 (4) 0.5 (5), 0.6 (6).

The sequence of phase transformations during synthesis in air of (1-x)$BaTiO_3$–$xLi_{0.5}Bi_{0.5}TiO_3$ was established by XRD analysis. The results of investigation (1-x)$BaTiO_3$–$xLi_{0.5}Bi_{0.5}TiO_3$ (x=0, 0.3) are presented in the Table. Table shows that a single-phase solid solution in (1-x)$BaTiO_3$–$xLi_{0.5}Bi_{0.5}TiO_3$ system forms at temperatures above 900ºC. With increasing x the formation temperature of solid solution decreases. Scheme of formation (1-x)$BaTiO_3$–$xLi_{0.5}Bi_{0.5}TiO_3$ solid solution is presented in Figure 4.

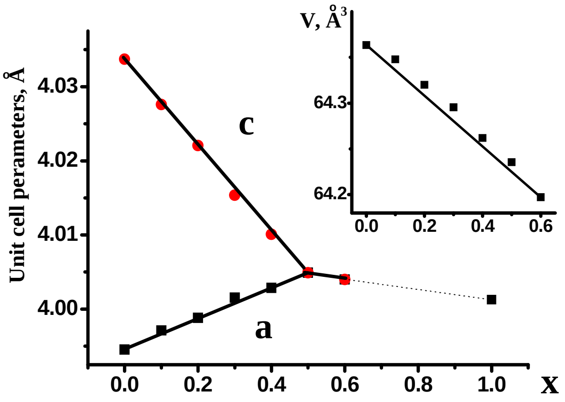

Fig. 3. The dependence of a and c parameters of (1-x)$BaTiO_3$–$xLi_{0.5}Bi_{0.5}TiO_3$ unit cell against x.

Interaction between the initial reactants (Li_2CO_3, $BaCO_3$, Bi_2O_3, TiO_2) begins at temperatures above 600°C. Phases $BaTi_4O_9$, $Bi_{12}TiO_{20}$ and Li_4TiO_4 are formed in the temperature range 600-650°C:

$$BaCO_3 + 4TiO_2 \xrightarrow{600-650^o C} BaTi_4O_9 + CO_2\uparrow;$$

$$6Bi_2O_3 + TiO_2 \xrightarrow{600-650^o C} Bi_{12}TiO_{20};$$

$$2Li_2CO_3 + TiO_2 \xrightarrow{600-650^o C} Li_4TiO_4 + 2CO_2\uparrow.$$

TABLE I. TABLE. PHASE COMPOSITION OF THE POWDERS IN THE $(1\text{-}x)BaTiO_3–x\ Li_{0.5}Bi_{0.5}TiO_3$ SYSTEM

T, °C	$x = 0$	$x = 0.3$
20-500	γ-$BaCO_3$, TiO_2	$BaCO_3$, TiO_2, Bi_2O_3, Li_2CO_3
600	γ-$BaCO_3$, TiO_2	$BaCO_3$, TiO_2, Bi_2O_3, Li_2CO_3, $BaTi_4O_9$, $Bi_{12}TiO_{20}$, Li_4TiO_4
650	γ-$BaCO_3$, TiO_2	$BaCO_3$, TiO_2, Bi_2O_3, Li_2CO_3, $BaTi_4O_9$, $Bi_{12}TiO_{20}$, Li_4TiO_4, $BaTiO_3$, $Bi_2Ti_2O_7$
700	γ-$BaCO_3$, TiO_2	$BaCO_3$, TiO_2, Bi_2O_3, Li_4TiO_4, $Li_4Ti_5O_{12}$, $Bi_4Ti_3O_{12}$, $BaTiO_3$, $Bi_2Ti_2O_7$
750	γ-$BaCO_3$, TiO_2	$BaCO_3$, TiO_2, Bi_2O_3, Li_4TiO_4, $Li_4Ti_5O_{12}$, $Bi_4Ti_3O_{12}$, $BaTiO_3$, $Bi_2Ti_2O_7$, $Bi_2Ti_4O_{11}$
800	γ-$BaCO_3$, TiO_2, $BaTiO_3$, $BaTi_3O_7$	$BaCO_3$, TiO_2, Bi_2O_3, Ba_2TiO_4, $Li_4Ti_5O_{12}$, $Bi_4Ti_3O_{12}$, $BaTiO_3$,
900	β-$BaCO_3$, TiO_2, $BaTiO_3$	TiO_2, Bi_2O_3, $Li_4Ti_5O_{12}$, $Bi_4Ti_3O_{12}$, $BaTiO_3$, $(1\text{-}x)BaTiO_3–xLi_{0.5}Bi_{0.5}TiO_3$
950	β-$BaCO_3$, TiO_2, $BaTiO_3$	TiO_2, Bi_2O_3, $Li_4Ti_5O_{12}$, $Bi_4Ti_3O_{12}$, $BaTiO_3$, $(1\text{-}x)BaTiO_3–xLi_{0.5}Bi_{0.5}TiO_3$
1000	TiO_2, $BaTiO_3$, Ba_2TiO_4,$BaTi_4O_9$	$(1\text{-}x)BaTiO_3–x\ Li_{0.5}Bi_{0.5}TiO_3$
1100	$BaTiO_3$, Ba_2TiO_4	$(1\text{-}x)BaTiO_3–x\ Li_{0.5}Bi_{0.5}TiO_3$
1200	$BaTiO_3$	$(1\text{-}x)BaTiO_3–x\ Li_{0.5}Bi_{0.5}TiO_3$

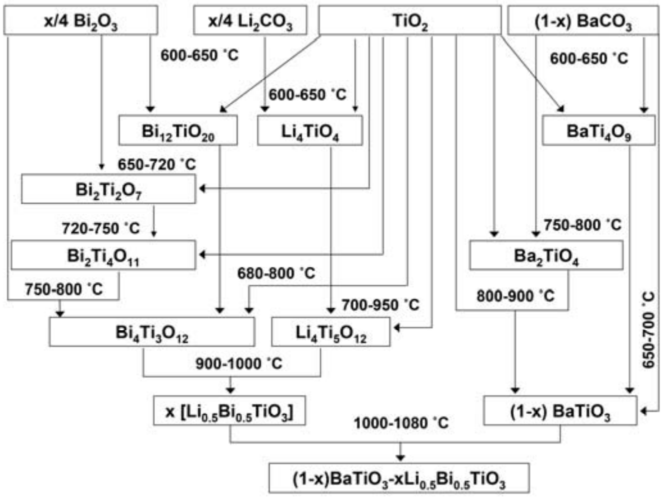

Fig. 4. Scheme of phase transformations sequence during solid state reaction synthesis of $(1\text{-}x)\ BaTiO_3–xLi_{0.5}Bi_{0.5}TiO_3$ (x=0.3) solid solution.

The formation of phases $Bi_4Ti_3O_{12}$, $Bi_2Ti_2O_7$, $Bi_2Ti_4O_{11}$ and $Li_4Ti_5O_{12}$ occurs with further increase in temperature according reactions:

$$Bi_{12}TiO_{20} + 8TiO_2 \xrightarrow{680–800^o C} 3Bi_4Ti_3O_{12};$$

$$Li_4TiO_4 + 4TiO_2 \xrightarrow{700–950^o C} Li_4Ti_5O_{12};$$

$$Bi_2O_3 + 2TiO_2 \xrightarrow{650–720^o C} Bi_2Ti_2O_7;$$

$$Bi_2Ti_2O_7 + 2TiO_2 \xrightarrow{720–750^o C} Bi_2Ti_4O_{11};$$

$$3Bi_2Ti_4O_{11} + 5Bi_2O_3 \xrightarrow{750–800^o C} 4Bi_4Ti_3O_{12};$$

$BaTiO_3$ phase formation is a multistep process:

$$2\ BaCO_3 + TiO_2 \xrightarrow{750–800^o C} Ba_2TiO_4 + 2CO_2\uparrow;$$

$$BaTi_4O_9 + 3BaCO_3 \xrightarrow{650–700^o C} 4BaTiO_3 + 3CO_2\uparrow;$$

$$Ba_2TiO_4 + TiO_2 \xrightarrow{800–900^o C} 2BaTiO_3.$$

Solid solution (1-x)BaTiO3–xLi0.5Bi0.5TiO3 begins to form at temperatures above 800°:

$$Li_4Ti_5O_{12} + Bi_4Ti_3O_{12} \xrightarrow{900–1000^o C} 8\ [Li_{0.5}Bi_{0.5}TiO_3].$$

$$(1\text{-}x)BaTiO_3 + x\ [Li_{0.5}Bi_{0.5}TiO_3] \xrightarrow{1000–1080^o C} (1\text{-}x)BaTiO_3–xLi_{0.5}Bi_{0.5}TiO_3$$

In $(1\text{-}x)BaTiO_3–xLi_{0.5}Bi_{0.5}TiO_3$, where $x = 0.3$, intermediate phase $BaTiO_3$ is formed at above 650°C, while an individual substance $BaTiO_3$ is formed at 1150°C. During the formation of the individual $BaTiO_3$, the presence of the intermediate phase $BaTi_3O_7$ at 800°C is also observed. The introduction of lithium-bismuth titanate reduces the sintering temperature of pure barium titanate. In particular, the sintering temperatures of the $(1\text{-}x)BaTiO_3–xLi_{0.5}Bi_{0.5}TiO_3$ solid solution are 1400ºC and 1300ºC at $x = 0$ and $x = 0.02$, respectively.

Temperature dependences of permittivity and dielectric loss tangent of $(1\text{-}x)BaTiO_3\text{-}xLi_{0.5}Bi_{0.5}TiO_3$ solid solutions are shown in Fig. 5. The increase in lithium-bismuth titanate content reduces the maximum of dielectric constant while the Curie temperature is remain constant for all x (T_C= 120ºC).

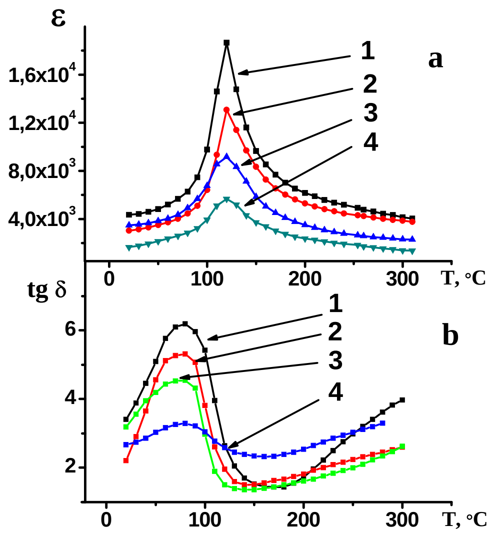

Fig. 5. Temperature dependence of permittivity (a) and dielectric loss tangent (b) of $(1\text{-}x)BaTiO_3\text{-}xLi_{0.5}Bi_{0.5}TiO_3$ ceramic, x = 0.1 (1); 0.15 (2); 0.2 (3); 0.3 (4). f = 100 kHz.

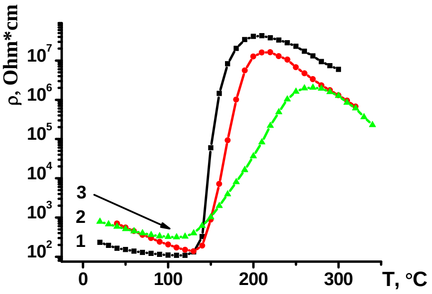

Fig. 6. Temperature dependence of resistance in ceramic (1-x)BaTiO$_3$-xLi$_{0.5}$Bi$_{0.5}$TiO$_3$, x = 0.1 (1) 0.2 (2) 0.3 (3).

Fig. 6 shows the temperature dependence of the resistivity for solid solutions (1-x)BaTiO$_3$-xLi$_{0.5}$Bi$_{0.5}$TiO$_3$. Lithium-containing solid solutions exhibit PTCR effect in the temperature range above 120ºC. With increase in lithium-bismuth titanate content, the temperature range of the PTCR effect increases, the maximum value of the resistance decreases, and the minimum resistance value increases. SEM shown that the average grain size in the (1-x)BaTiO$_3$-xLi$_{0.5}$Bi$_{0.5}$TiO$_3$ varies from 6 μm (x=0.1) to 0.5 μm (x = 0.6). Increase in resistance with increasing x may be associated with a decrease in the ceramic grain size.

TEM of (1-x)BaTiO$_3$-xLi$_{0.5}$Bi$_{0.5}$TiO$_3$ solid solutions shown that ferroelectric domains are visible in the perovskite grains (Fig. 7). Electron diffraction data confirm the formation of crystalline perovskite structure. It has been shown that grain boundaries are free from additional phases. The chemical compositions of grain boundary and core were studied by EDX analysis. The chemical composition of the core and the grain boundary of ceramics satisfy (1-x)BaTiO$_3$-xLi$_{0.5}$Bi$_{0.5}$TiO$_3$ solid solutions. It was found that the grain boundary (Fig. 7b) enriched by bismuth and oxygen compared with the core of grain (Fig. 7c), while other elements are uniformly distributed along the ceramic grain.

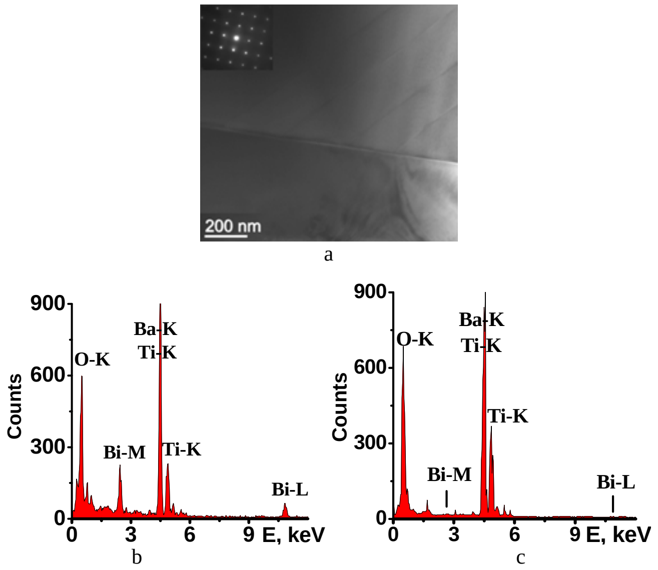

a

b

c

Fig. 7. TEM of grain boundary (a) and EDX spectra of boundary (b) and the core (c) of ceramic grain 0.8BaTiO$_3$-0.2Li$_{0.5}$Bi$_{0.5}$TiO$_3$ sample.

EDX studies conclude that in the core of grains, the oxygen ions is lost during the sintering, oxygen vacancies are formed and part of Ti^{4+} reduces its oxidation state Ti^{4+} → Ti^{3+}:

$$\begin{gathered}(Ba^{2+}_{1-x}Na^{+}_{x/2}Bi^{3+}_{x/2})Ti^{4+}O_3+\frac{1}{2}H_2\rightarrow\\(Ba^{2+}_{1-x}Na^{+}_{x/2}Bi^{3+}_{x/2})(Ti^{4+}_{1-y}Ti^{3+}_{y})O_{3-\delta}+H_2O\end{gathered}\tag{2}$$

Therefore, the semiconductor properties are formed due to oxygen losses, but not due excess charge compensation as in donor doped barium titanate.

At grain boundaries, oxygen vacancies are filled resulting in greater oxygen concentration at grain boundary:

$$\begin{gathered}(Ba^{2+}_{1-x}Na^{+}_{x/2}Bi^{3+}_{x/2})(Ti^{4+}_{1-y}Ti^{3+}_{y})O_{3-\delta}+\frac{1}{2}\delta O_2\rightarrow\\(Ba^{2+}_{1-x}Na^{+}_{x/2}Bi^{3+}_{x/2})Ti^{4+}O_3\end{gathered}\tag{3}$$

Oxygen diffusion at grain boundaries also accompanied with inverse change in titanium oxidation state (Ti^{3+} → Ti^{4+}) and formation of dielectric layers.

IV. CONCLUSIONS

Semiconductor solid solutions of the system (1-x)BaTiO$_3$–xLi$_{0.5}$Bi$_{0.5}$TiO$_3$ were synthesized by solid state reaction technique. It was shown that the formation of solid solutions occurs in the limited range $0 \le x \le 0.6$. Introduction of lithium-bismuth titanate significantly reduces the sintering temperature of barium titanate. It was found that with increasing lithium-bismuth titanate content, unit cell volume decreases and structure changes from tetragonal to cubic symmetry due to decrease in the average ionic radius in barium site. The unit cell parameter of unstable cubic Li$_{0.5}$Bi$_{0.5}$TiO$_3$ was determined (a=4.00126 Å). It was found that increase in x in (1-x)BaTiO$_3$–xLi$_{0.5}$Bi$_{0.5}$TiO$_3$ solid solutions does not change the Curie temperature. It was shown that (1-x)BaTiO$_3$–xLi$_{0.5}$Bi$_{0.5}$TiO$_3$ materials exhibit PTCR effect. Increase in x increases the minimum resistance value in PTCR region. It was found that the PTCR effect of lithium-containing materials is caused by the presence of semiconductor core and dielectric grain boundaries.

REFERENCES

[1] W. Maison, R. Kleeberg, R. B. Heimann, S. Phanichphant J. Eur. Ceram. Soc. 23 (2003) 127–132.

[2] M. Okazaki, Barium Titanate Semiconductors. Ed. Moscow. Energoizdat (translated from Japanese). 1982, 328 p.

[3] Z.C. Li, B. Bergman, Ceramics International. 31 (2005) 375–378.

[4] S. Leng, G. Li, L. Zheng, T.Wang, J. Am. Ceram. Soc. 92 (2009) 2772–2775.

[5] M. Chen, Q. Xu, B.H. Kim, B. Ahn, J. Eur. Ceram. Soc. 28 (2008) 843–849.

[6] D. Lin, D. Xiao, Materials Letters. 58 (2004) P. 615–618.

[7] X. Jiang, Q. Yang, Z. Yu, F. Hu, C. Chen, N. Tu, Y. Li J. Alloys and Compounds. 493 (2010) 276–280.

[8] N. Lei, M. Zhu, L. Wang, P. Yang, Y. Hou, Phys. Status Solidi A. 208 (2011) 186–190.

[9] Y. Pu, J. Wei, Y. Mao, J. Wang, J. Alloys and Compounds. 498 (2010) L5– L7.

[10] L.K. Templeton, J.A. Pask, J. Am. Ceram. Soc., 42 (1959) 212–216.

[11] J. C. JR. Mikkelsen, J. Am. Ceram. Soc. 63 (1980) 331–335.

[12] V. M. Goldschmidt, Die Naturwissenschaften. 14 (1926) 477–485.